

## THREE-DIMENSIONAL SPONTANEOUS MAGNETIC RECONNECTION

ANDREY BERESNYAK

Naval Research Laboratory, Washington, DC 20375

*Draft version June 8, 2021*

### ABSTRACT

Magnetic reconnection is best known from observations of the Sun where it causes solar flares (Sweet 1969; Parker 1957; Dungey 1961). Observations estimate the reconnection rate a small, but non-negligible fraction of the Alfvén speed, so-called fast reconnection. Until recently, the prevailing pictures of reconnection were referring to either resistivity or plasma microscopic effects, which was contradictory to the observed rates. The alternative picture was either reconnection due to the stochasticity of magnetic field lines in turbulence (Lazarian & Vishniac 1999) or the tearing instability of the thin current sheet (Biskamp 1986; Loureiro et al. 2007). In this paper I simulated long-term three-dimensional nonlinear evolution of a thin, planar current sheet subject to fast oblique tearing instability using direct numerical simulations of resistive-viscous MHD. The late-time evolution resembles generic turbulence with  $-5/3$  power spectrum and scale-dependent anisotropy, so I conclude that the tearing-driven reconnection becomes turbulent reconnection. The turbulence is local in scale, so microscopic diffusivity should not affect large-scale quantities. This is confirmed by convergence of the reconnection rate towards  $\sim 0.015v_A$  with increasing Lundquist number. In this spontaneous reconnection with mean field and without driving the dissipation rate per unit area also converge to  $\sim 0.006\rho v_A^3$ , the dimensionless constants 0.015 and 0.006 are governed only by self-driven nonlinear dynamics of the sheared magnetic field. Remarkably, this also means that thin current sheet has a universal fluid resistance depending only on its length to width ratio and to  $v_A/c$ .

*Subject headings:* magnetohydrodynamics—particle acceleration

### 1. INTRODUCTION

Current sheets are abundant in magnetized plasmas. Similar to thin vortices of hydrodynamics, they are naturally created by the nonlinear evolution of the conductive fluid (Parker 1994; Biskamp 2000; Priest & Forbes 2000). Magnetic X-points naturally evolve into current sheets due to currents mutual attraction, creating the so-called Y-point configuration (Fig. 1). Perhaps one of the most conspicuous phenomenon associated with current sheets in plasmas are solar flares, the bursts of radiation of up to  $6 \times 10^{33}$  ergs in X-rays. Following the big solar flare, the coronal mass ejections (CME) occurs, hinting to the global rearrangement of the magnetic field, which is called magnetic reconnection. Another well-known process is a magnetospheric storm, which is a perturbation of magnetosphere, associated with reconnection in the magnetotail. While CME demonstrates that there was a topological rearrangement of the magnetic field, the careful observations near the flare site typically estimate the rate of inflow of magnetic field lines, called reconnection rate, to a 0.001 – 0.1 fraction of the Alfvén speed  $v_A = B/\sqrt{4\pi\rho}$  (see, e.g., Dere 1996).

In a well-conductive plasma, one might expect that current sheets are non-dissipative and, therefore, invisible. Indeed, the Sweet-Parker (SP) model (Sweet 1969; Parker 1957) predicts very low reconnection rate for most astrophysical and space magnetic configurations. The dimensionless number characterizing plasma conductivity is the Lundquist number  $S = Lv_A/\eta$ , where  $L$  is the length of the layer  $\eta$  is magnetic diffusivity. High Lundquist number means the magnetic resistive decay time,  $L^2/\eta$ , is much larger than Alfvén crossing time,  $L/v_A$ . For laminar thin current sheets, the Sweet-Parker

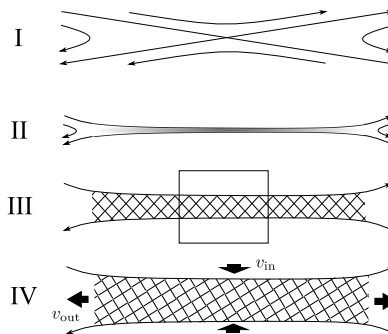


FIG. 1.— A cartoon of high-Lundquist number magnetic reconnection. Magnetic X-point (I) collapses into a thin current sheet, (II), which goes unstable and produces turbulent current layer (III), expanding with reconnection rate  $v_r$ , until it develops an outflow and reach quasi-stationary state (IV). Our paper discusses (III), we simulate a zoom-in of the current layer in a box which initially appear as a planar current layer.

(SP) model (Sweet 1969; Parker 1957) predicts reconnection rate of  $v_A/\sqrt{S}$ , this enhancement compared to resistive diffusion is due to the fact that magnetic field diffuses only through a thin width of the current sheet  $L/\sqrt{S}$ . This speed, however, is extremely low for most astrophysical and space magnetic configurations. The SP model, in the limit of very high  $S$ , becomes consistent with the so-called frozen-in condition of the ideally conductive fluids. The SP prediction, therefore, contradicts the idea that the discontinuity in the magnetic field may result in an arbitrary reconnection rate independent on resistivity, as in the Syrovatskii’s model (Syrovatskii 1971). The search for fast reconnection have shifted towards microscopic effects beyond MHD, e.g. effects in collision-

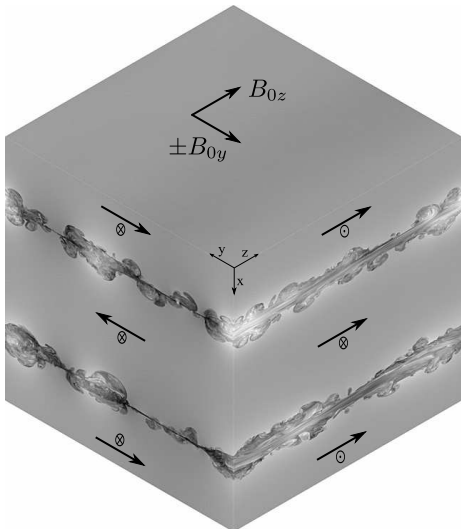


FIG. 2.— This figure demonstrates the all-periodic box reconnection setup with two current layers, reconnecting field  $\pm B_{y0}$  and the imposed mean field  $B_{z0}$ , the magnitude of  $B$  is shown as grayscale on the surface of the box.

less plasmas (Drake et al. 2006; Daughton et al. 2011; Che et al. 2011). Alternative approaches suggested that in presence of turbulence the magnetic field lines will be stochastic (Lazarian & Vishniac 1999; Kowal et al. 2009; Eyink et al. 2011, 2013) which would lead to fast reconnection, which have implications for particle acceleration (Lazarian et al. 2008; Beresnyak & Lazarian 2015; Beresnyak & Li 2016). The study of the resistive tearing instability in the thin current sheet (Biskamp 1986), surprisingly resulted in a conclusion that it becomes faster and not slower with decreasing resistivity (Loureiro et al. 2007; Huang & Bhattacharjee 2010; Loureiro et al. 2012) at sufficiently high  $S$ . It has become clear that SP model is problematic at high  $S$  because thin SP current sheets are unstable above the critical Lundquist number  $S = Lv_A/\eta \sim 10^4$ . In a two-dimensional (2D) resistive reconnection scenario, secondary instability of the current sheet between magnetic islands will result in a resistivity-independent reconnection (Uzdensky et al. 2010). The two-dimensional (2D) MHD simulations measured reconnection speeds around  $0.01 \div 0.03v_A$  (Loureiro et al. 2012; Huang & Bhattacharjee 2010) and observed hierarchical formation and ejection of plasmoids. Plasma simulations demonstrated that collisionless thin current layers are also unstable (Daughton et al. 2009).

In this paper I did three-dimensional (3D) simulations of thin current sheet with significant imposed mean field, starting with oblique tearing and developing into nonlinear phase which I called spontaneous turbulent reconnection.

In what follows Section 2 describes simulation setup, Section 3 overview the results of simulations in terms of bulk average quantities, such as total energy budget and its evolution, Sections 4 and 5 describes local properties of turbulence, spectrum and anisotropy. Section 6 comments on the global nature of the perturbation of the magnitude of the magnetic field (slow mode). Section 7 discusses in some detail the differences in reconnection picture in 2D and 3D cases. Section 8 proposes phe-

TABLE 1  
SPONTANEOUS RECONNECTION MHD EXPERIMENTS

Run	$N^3$	Dissipation	$S$ or $S_A^{0.4}$	$B_{y0}/B_{z0}$	$v_r/v_A$
N1	$576^3$	$-3.6 \cdot 10^{-4} k^2$	$1.7 \times 10^4$	1.0	0.0124
H1B1	$576^3$	$-2.4 \cdot 10^{-9} k^4$	$2.5 \times 10^4$	0.5	0.0214
H1B2	$576^3$	$-2.4 \cdot 10^{-9} k^4$	$2.5 \times 10^4$	1.0	0.0210
H1B3	$576^3$	$-2.4 \cdot 10^{-9} k^4$	$2.5 \times 10^4$	2.0	0.0187
N2	$768^3$	$-2.5 \cdot 10^{-4} k^2$	$2.5 \times 10^4$	1.0	0.0117
H2	$768^3$	$-9.4 \cdot 10^{-10} k^4$	$3.7 \times 10^4$	1.0	0.0183
N3	$1152^3$	$-1.4 \cdot 10^{-4} k^2$	$4.4 \times 10^4$	1.0	0.0155
H3	$1152^3$	$-9.7 \cdot 10^{-10} k^4$	$3.6 \times 10^4$	1.0	0.0146
N4	$1536^3$	$-9.8 \cdot 10^{-5} k^2$	$6.4 \times 10^4$	1.0	0.0154
H4	$1536^3$	$-3.7 \cdot 10^{-10} k^4$	$5.4 \times 10^4$	1.0	0.0144

nomenological model for the reconnection rate. Section 9 discusses implications for particle acceleration, Section 10 points out that thin current layer could be viewed from electromagnetic viewpoint as having non-zero resistance per unit length, even in the limit of vanishing resistivity. Section 10 is a Discussion.

## 2. PROBLEM SETUP

One of the simplest setups to study nonlinear development of tearing is a periodic setup with the mean field  $B_{z0}$  threading the box, reconnecting field  $\pm B_{y0}$  changing sign in the  $x$  direction. I also consider incompressible case, in which situation the problem has only two defining dimensionless numbers: 1) the Lundquist number  $S$  2) the ratio  $B_{y0}/B_{z0}$ .

This very simple geometry physically corresponds to the initial (albeit already nonlinear) development of tearing before the outflow becomes important. The cartoon on Fig. 1 illustrates the typical progression of high- $S$  spontaneous reconnection by showing a cut perpendicular to the current and global mean field direction: magnetic configuration with the X-point (I) may develop into the thin current sheet (II), the latter develops instability, the instability goes nonlinear and produces turbulent current layer (III) which later expands and produces classic picture with inflow and outflow (IV). I studied the initial regime before the outflow becomes important, designated as regime III on Fig. 1, which is especially interesting because it has highest volumetric dissipation rate.

I used all-periodic setups, so I actually simulated two current layers, and all the results is the average between the properties of these two layers. Fig. 2 demonstrates the setup and shows the simulation snapshot during the development of the nonlinear phase, with the magnitude of  $B$  is shown by grayscale on the surface of the box. One of the numerical challenges in studying 3D spontaneous reconnection was to break through the critical Lundquist number barrier of  $10^4$ , which require sufficiently big boxes. In simulations with imposed large-scale perturbation, such as Daughton et al. (2011); Oishi et al. (2015); Huang & Bhattacharjee (2016) the Lundquist number is directly estimated using the size of the perturbation, which is typically the box size. In these cases simulations try to reproduce the whole current layer in a Sweet-Parker configuration in regime IV of Fig. 1. I, on the other hand, try to simulate a zoom-in of the middle of the current layer in regime III which

initially look like a planar current sheet but at later times will develop large scale perturbations. If I define Lundquist number using the box size, as  $S = v_{Ay}L/\eta$ , and the system size  $L_S$  is actually bigger than the zoom-in box size, the Lundquist number of the whole system  $S_S = v_{Ay}L_S/\eta$  is larger than  $S$  which I quote in Table 1. I can, therefore, safely assume that the larger system is unstable to tearing, just as my planar current sheet is unstable. A subtle difference of these two types of setup is that the simulations with global large-scale initial perturbations aim to describe stationary regime IV at later times,  $t \gg L_S/V_A$ , with a finite, albeit large,  $S$ , while my planar current sheet setup aim to simulate earlier times,  $t < L_S/V_A$ , when the global outflow did not have time to form yet. I also assume that  $L_S \gg L$  i.e. the global Lundquist number  $S_S$  is asymptotically large, so I can ignore gradients from the large-scale setup of the system and only impose small-scale perturbations. The end time of my simulations was determined by the development of large-scale structures, as long as these structures become comparable with the box size, the box size deemed not sufficient, similarly to simulations of nonlinear Kelvin-Helmholtz instability.

I used pseudospectral code with explicit dissipation coefficients – viscosity and magnetic diffusivity, equal to each other. The code solves incompressible resistive-viscous MHD equations, does not have inherent dissipation or dispersion grid errors and is mostly described in (Beresnyak 2014), except in the present paper I used full MHD, not reduced MHD. These simulations are DNS, e.g. they are well-resolved with the dimensionless maximum wavenumber satisfying  $k_{\max}l_\eta > 1$ , where  $l_\eta = (\eta^3/\epsilon)^{1/4}$  is the dissipation (Kolmogorov) scale<sup>1</sup>.

Normal viscosity and magnetic diffusivity  $\eta\nabla^2B$  was used in one series of simulations and the hyper-diffusivity of the fourth order,  $\eta_4\nabla^4B$  in the other. The Lundquist number was defined in terms of the box size  $L = 2\pi$  and the reconnecting field  $v_{Ay} = 1$  as  $S = v_{Ay}L/\eta$  and the hyper-Lundquist number as  $S_4 = v_{Ay}L^3/\eta_4$ . The Lundquist number  $S$  and the hyper Lundquist number  $S_4$  that give the same dynamical range of scales between dissipation scale and outer scale, e.g. the ratio  $L/l_\eta$ , are related by  $S = S_4^{4/10}$ , assuming Kolmogorov scaling. The rationale behind the two dissipation schemes was to check the influence not only on  $S$ , but also on the dissipation functional form to the bulk quantities, such as reconnection and dissipation rate. The magnetic Prandtl number was unity:  $Pr_m = \nu/\eta = 1$ , which was motivated by the desire to reach the highest possible  $S$  while staying well-resolved. As I will show below, the amount of magnetic and kinetic dissipation were close to each other, which is typical for an ordinary MHD cascade.

The simulations were set up with a thin current sheet with Harris profile and seeded with small initial perturbations,  $\sim 10^{-6}$  of the magnetic energy. These perturbations subsequently evolved due to oblique tearing near the current sheet itself, the bulk of the volume was almost undisturbed. At later times this evolved into fully nonlinear turbulent current layer. The boundary between

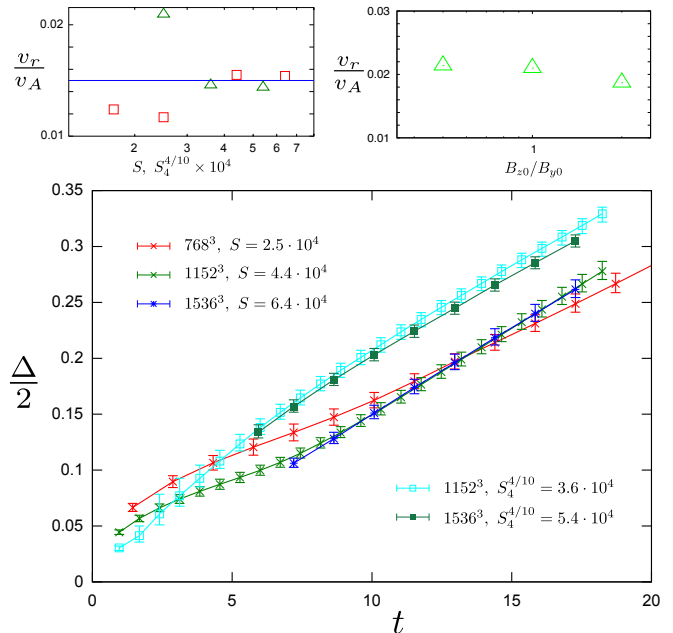


FIG. 3.— The time evolution of the current layer width  $\Delta$  (bottom) and the inferred reconnection speed as a function  $S$  (top left) and the ratio of  $B_{z0}/B_{y0}$  (top right). The error bars were obtained by varying the current density threshold by a factor of two. The difference in the initial evolution of hyper- and normal-diffusion cases is due to much faster development of hyper-resistive oblique tearing compared to normal oblique tearing. The variation of  $v_r$  around  $\sim 13\%$  with  $B_{z0}/B_{y0}$  varying by a factor of 4 and was within measurement error.

the undisturbed volume, which had nearly zero current and the turbulent current layer was fairly well-defined, as shown on Fig. 2. The inside of the current layer was determined as opposite to the undisturbed fluid where current density is always small. The point at which the current density exceeds a certain threshold in magnitude was regarded as the beginning of the current layer. I varied current density thresholds to study the dependence on the measurement of the layer width  $\Delta$ . The procedure to obtain the errors for that measurement was to vary the lower and upper thresholds for current by a factor of two. The list of all simulations is presented on Table 1.

### 3. EVOLUTION

The evolution of the current layer width and the inferred reconnection rate are shown on Fig. 3. The system initially contained the energy density of the opposing field  $B_{y0}^2/8\pi$ , which was free to dissipate and the energy density of the mean imposed field  $B_{z0}^2/8\pi$ , which had to conserve due to conservation of total flux through x-y plane. After subtracting the latter contribution, a I designate a dimensionless free energy density as

$$w = (4\pi\rho v^2 + B^2 - B_{z0}^2)/B_{y0}^2, \quad (1)$$

which is unity in the undisturbed fluid. After  $t \approx 2$  turbulence in the layer fully develops, and the average  $w$  within the layer,  $w_t \approx 0.6$ , while the undisturbed part still have  $w = 1$ . The dissipation of  $w_d \equiv 1 - w_t = 0.4$  fraction of energy happens during development of turbulence and stays approximately constant.

<sup>1</sup> Moderately under-resolved cases exhibit visible ringing at grid scale, which happened in simulation H2 (Table 1), this simulation wasn't included in the reconnection rate measurements.

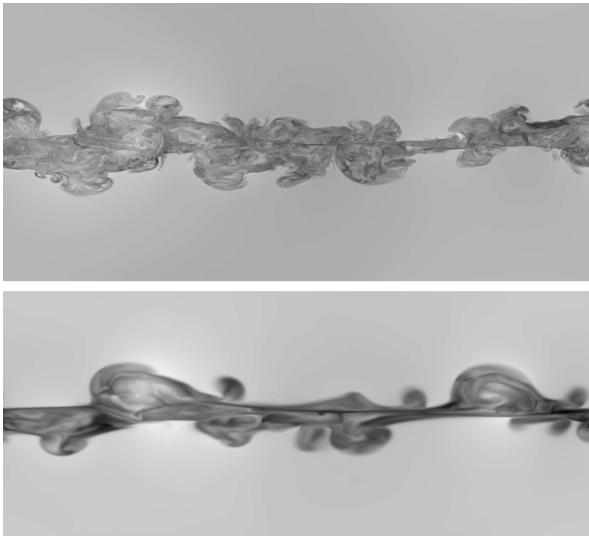


FIG. 4.— Zoom-in  $x$ - $z$  slices of the turbulent current layer. Mean magnetic field is out of the plane. Upper part is the magnitude of  $B$  in hyper-viscous simulation, lower part – in viscous simulation.

I inferred reconnection rate as the growth speed of the current layer width  $v_r = d\Delta/dt$ . This is different from a conventional definition as an inflow speed in stage IV (Fig. 1). In stage III, however it is a meaningful definition, in terms of how much free magnetic energy is available to the system per unit time per unit area of the current layer. From this energetic viewpoint inflow definition and my definition are similar.

$V_r$  was around  $0.015v_{Ay}$  for high Lundquist numbers and appear to be only weakly dependent on the imposed mean field  $B_{z0}$  (Fig. 3). The dissipation rate per unit area from both sides of the current sheet (note a factor of two) can be calculated from  $w_d$  and  $v_r$  as

$$\epsilon_S = 2w_d v_r (1/2)\rho v_{Ay}^2 \approx 0.006\rho v_{Ay}^3, \quad (2)$$

note that conventional dissipation rate per unit mass, traditionally used in theory of incompressible turbulence will be expressed using current layer width  $\Delta$  as

$$\epsilon = (1/\rho)\epsilon_S/\Delta = w_d v_r v_{Ay}^2/\Delta, \quad (3)$$

and will depend on time. The turbulence in the expanding current layer is not stationary turbulence in a sense that it grows in volumes and produces turbulent energy as well as dissipates energy. The outer scale of this turbulence also grows in time.

The contribution to turbulent fraction of the energy density  $w_t \approx 0.6$  was partitioned to  $\sim 0.55$  in  $x$  and  $y$  magnetic component,  $\sim 0.02 - 0.04$  in  $\delta B_z$  component and  $\sim 0.01 - 0.02$  in kinetic energy. The turbulence in the current layer was strongly anisotropic with respect to  $B_{z0}$  direction, with wavevector predominantly perpendicular to  $z$ . The  $B_x$  and  $B_y$  components, carrying most of the energy, therefore, represented Alfvénic perturbations, while the sub-dominant  $\delta B_z$  was the slow-mode (pseudo-Alfvén) perturbation. I discuss anisotropy in more detail in Section 6, noticing that the fact that the reconnection rate depends only weakly on  $B_{z0}$  is not surprising, since the anisotropic turbulence of Alfvénic perturbations also known as Alfvénic turbulence or reduced MHD turbu-

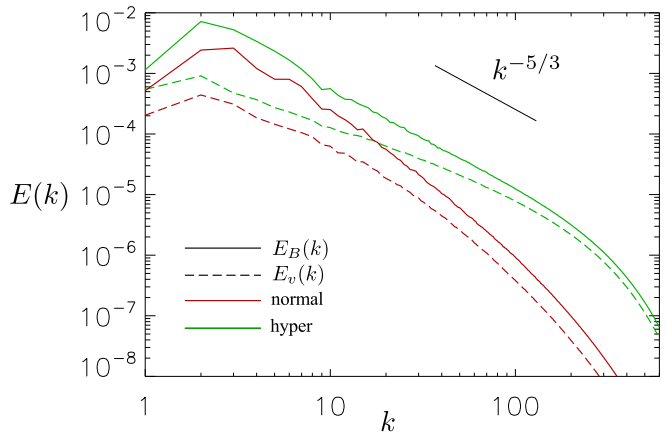


FIG. 5.— The  $y$ - $z$  power spectra of velocity and magnetic field for simulations N4 and H4. The spectral slopes were around  $-1.5 \div -1.7$ , which is characteristic of local-in-scale turbulence.

lence possesses rescaling symmetry with respect to  $B_{z0}$  (Beresnyak 2012), which I actually confirm in Section 6. The domination of Alfvénic perturbations in reconnection with strong mean field is extremely important as it sheds light to fluid-like behavior in plasma simulations, e.g. (Daughton et al. 2009), in spite of significant collisionless effects. The explanation for this is that reduced MHD is well-applicable to collisionless plasmas on scales above ion Larmor radius  $r_L$ , and that plasma does not require significant collisional terms to behave like reduced MHD fluid (Schekochihin et al. 2009).

#### 4. SPECTRA

The structure of the perturbed current layer looked rather turbulent (Fig. 4) with only a small fraction of the initial current sheet structure being retained.

I defined the power spectra of turbulent perturbations in the  $yz$  plane as

$$E(k_l) = L^{-1} \int \hat{f}(\mathbf{k}_l) \hat{f}^*(\mathbf{k}_l) d\phi dx \quad (4)$$

where  $k_l = (k_y, k_z)$  – a wavevector in  $yz$  plane,  $\hat{f}(\mathbf{k}_l)$  – Fourier transforms of either  $v$  or  $B$ . Neglecting  $k_x$  in this spectrum is necessary to get rid of the contribution from  $\pm B_{y0}$  jump across the current layer which happens in the  $x$  direction. The spectrum, presented on Fig. 5 has magnetic contribution dominating over kinetic on large scales, but tend to approximate equipartition on smaller scales. This is not surprising, since turbulence is driven by magnetic energy. This spectral picture, qualitatively, is characteristic for decaying magnetic turbulence, including cases when initial field was completely random (see, e.g. Biskamp 2003; Brandenburg et al. 2015).

The total energy spectral slope was around  $-1.5 \div -1.7$ , roughly consistent with Goldreich-Sridhar (Goldreich & Sridhar 1995) scaling. The slopes between  $-1$  and  $-3$  are indicative of local-in-scale turbulence. Precise measurement of the spectral slope in these simulations was difficult due to limited inertial range, however, the scale-locality would imply that at sufficiently high  $S$  the inertial range scaling and anisotropy will be the same as in the homogeneous driven MHD turbulence. In the next section I test the

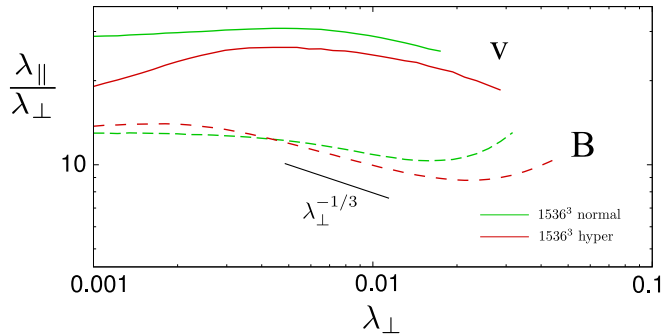


FIG. 6.— Anisotropy of velocity and magnetic perturbations in the current layer measured with respect to the local field. I used conditional 2-point structure function where both points were within the current layer. The high anisotropy, especially for the velocity field, is due to low amplitude of velocity perturbations and approximately corresponds to the critical balance between parallel and perpendicular timescales.

anisotropy component of this conjecture.

The scale-locality is a key ingredient in theories of turbulent reconnection. Indeed full scale-locality will imply that large-scale quantities, such as reconnection rate and dissipation rate per unit area should be independent on any microphysics. Speaking in practical terms, if both ion Larmor radius  $r_L$  and ion skip depth  $d_i$  are much smaller than the minimum size of the problem – the layer width  $\Delta$ , reconnection rate will be independent on microphysics. Note that in regime (IV), stationary reconnection,  $\Delta$  will become constant around  $0.015L^2$ . This allows us to estimate the range of applicability of this particular mechanism of fast reconnection.

## 5. ANISOTROPY

I have calculated second-order structure functions of the turbulent  $v$  and  $B$  fields inside the current layer, e.g. for velocity:

$$SF_v^2(l_{\parallel}, l_{\perp}) = \langle (v(\mathbf{r} - \mathbf{l}) - v(\mathbf{r}))^2 \rangle_{\mathbf{r}}. \quad (5)$$

Note that I assumed that it depends only on the component of  $\mathbf{l}$  parallel and perpendicular to the magnetic field. Two types of such measurement are possible: when parallel direction is determined by the global mean magnetic field, in my case  $z$  direction, or local magnetic field  $\mathbf{B}$ . Scale-dependent anisotropy of Goldreich & Sridhar (1995) model is observed with the local measurement (see, e.g., Cho & Vishniac 2000; Beresnyak & Lazarian 2009).

Using these structure functions for  $v$  and  $B$  I built correspondence between  $\lambda_{\parallel}$  and  $\lambda_{\perp}$  by equating SF values in parallel and perpendicular direction. More details on this type of measurement can be found in Beresnyak & Lazarian (2009). Fig. 6 shows anisotropy  $\lambda_{\parallel}/\lambda_{\perp}$  as a function of  $\lambda_{\perp}$ . One thing to notice is that the value of anisotropy in this particular simulation, with  $B_y/B_z = 1$ , is around 20. At the same time the RMS value of velocity perturbation is around  $0.08 - 0.11v_{Ay}$ . The interaction strength parameter  $\xi = \delta v \lambda_{\parallel} / v_A \lambda_{\perp}$  will be around unity, i.e. these perturbations are, approximately, “critically balanced”. This means that from

<sup>2</sup> Assuming reconnection rate is  $0.015v_A$  in regime IV, see also simulations with outflow, e.g. Loureiro et al. (2012).

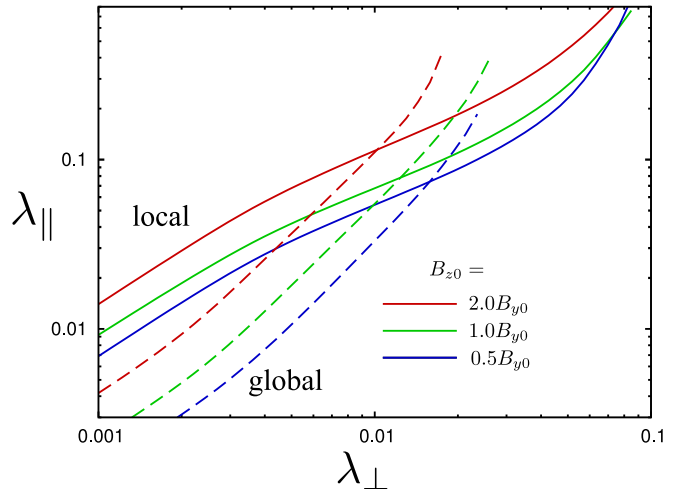


FIG. 7.— Comparison of anisotropies in simulations with different imposed field. Solid lines – measurement with respect to the local field, dashed lines – measurement with respect to the  $z$  direction. We expect symmetry  $\lambda_{\parallel}/B_{z0} = const$  in the limit of  $B_{z0} \gg B_{y0}$  for the measurement with respect to  $z$  direction (RMHD symmetry). This symmetry is well satisfied between  $B_{z0} = 2.0B_{y0}$  and  $B_{z0} = 1.0B_{y0}$  cases, but not so well satisfied between  $B_{z0} = 1.0B_{y0}$  and  $B_{z0} = 0.5B_{y0}$  due to the fact that  $B_{z0}/B_{y0}$  is not asymptotically large.

MHD perspective we are dealing with “strong” turbulence, i.e. nonlinear interaction terms have the same contribution as the tension of the mean field  $B_z$ . Also note that this anisotropy corresponds to the angle of the field line bending  $\sim 1/20$  which is much smaller than the angle of the initial stripes of developing oblique tearing ( $45^\circ$  in the case of  $B_y/B_z = 1$ ). So the turbulence self-organizes itself into being strong and forgets properties of the oblique tearing that initiated it.

The evidence for scale-dependent anisotropy is only tentative, considering rather short inertial range, the expected law of scale-dependency from Goldreich & Sridhar (1995) is  $\lambda_{\parallel}/\lambda_{\perp} \sim \lambda_{\perp}^{-1/3}$ , see Fig. 6.

Another important indicator is how anisotropy varies with the value of the mean field  $B_{z0}$ , this is presented on Fig. 7. I plotted both local and global anisotropy measurements. Note how  $\lambda_{\parallel}$  measurements have the same shape and are increasing with increasing  $B_{z0}$ . In a purely Alfvénic dynamics, also called reduced MHD,  $\lambda_{\parallel}$  is strictly proportional to  $B_{z0}$  (see, e.g., Beresnyak 2012). I noticed that this scaling is almost perfect between  $B_{z0} = 1$  and  $B_{z0} = 2$  cases, which further confirms that Alfvénic dynamics dominates in the current layer turbulence.

## 6. DIAMAGNETISM

In the  $B_{y0}/B_{z0} = 1$  case, apart from Alfvén mode, which contained 93% in total energy of turbulent motions, the rest 7% are perturbations in  $B_z$ . These perturbations are strongly anisotropic and this component represents pseudo-Alfvén or slow mode. The perturbations are energetically dominated by large scales and have a well-defined global structure: namely the perturbation is negative (decreasing  $B_z$ ) on the edge of the layer and positive (increasing  $B_z$ ) in the middle of the layer, see

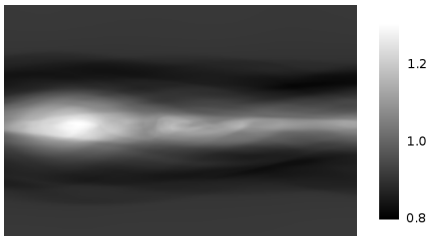


FIG. 8.— Zoom in of  $B_z$  averaged over  $z$  in the  $x$ - $y$  plane for simulation with  $B_{z0}/B_{y0} = 1$ . The width of the picture, along  $y$ , is  $0.4L$ . In strongly anisotropic perturbations this component represents pseudo-Alfvén or slow mode.

Fig. 8. Note that total  $B_z$  flux must conserve. Why turbulence creates large-scale structure in  $B_z$  so that it is larger in the center? This could be due to the diamagnetism of turbulence, which is stronger on the edge, where turbulence is more intense, so that the diamagnetism of turbulence has been pushing  $B_z$  flux towards the center. This conjecture will require future research. The peculiar structure of the mean flux through the layer can have consequences for the particle acceleration in turbulent current layers as particles are more likely to be trapped in the low- $B_z$  regions. When the mean field increases, the effect becomes negligible due to weaker coupling between Alfvén and slow mode.

## 7. 2D VS 3D

The results reported above appear to be qualitatively different from previous 2D results, which was expected: the geometrical constraints in the 2D magnetic configuration naturally features magnetic separatrices, X-points and magnetic islands, which are normally absent in 3D. Also, the dynamic influence of the global mean field, which is present in a generic reconnection geometry, is completely ignored by the 2D treatment. Another important point is that if  $B_z$  tension plays no important role in 2D, the perturbations that govern 2D case are not Alfvénic and the arguments for the reduced MHD analogy I used in the above section are also not applicable.

The 3D spontaneous reconnection that I studied here, proceeded in a different way than the 2D case, which, in Loureiro et al. (2012) was dominated by the ejection of plasmoids and had significant time-dependence. In the 3D case, considered here, I observed a very steady rate (Fig. 3) with turbulent current layer slowly eating through the mostly undisturbed fluid and turbulence being fueled by the free energy of the oppositely directed magnetic fields. 3D case was also different from 2D case in that the memory of the initial conditions, i.e. the location of the original current sheet was largely forgotten. In 2D case the current sheet remains precisely where it was, up to very high  $S$ , generating and ejecting plasmoids along the same line. In 3D case only small pieces of the original current sheet are visible after  $t = 10$  and the layer otherwise looks turbulent. Few large-scale structures in 3D may be called flux ropes, however, unlike 2D, they are turbulent inside (Fig. 4), also the number of these structures does not depend on  $S$  as it does in 2D case described in Uzdensky et al. (2010). Another difference with 2D is the asymmetry of emerging turbulence with respect to the original current sheet – in 3D often

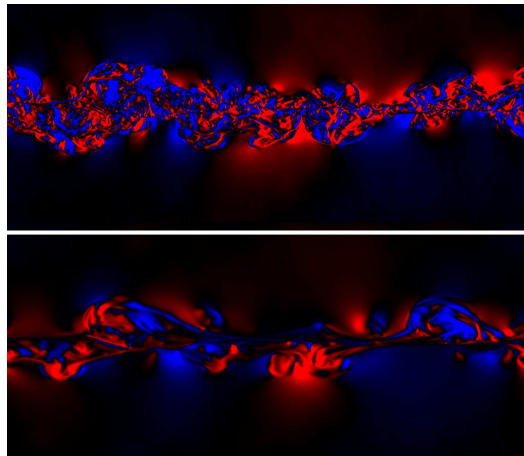


FIG. 9.— The structure of  $v_x$  in the  $x$ - $y$  slice of the layer. The width of the picture is the box size. Red and blue show positive and negative  $v_x$ , for the same slices as on figure above. The turbulent current layer generally lacks the bipolar inflow symmetry of the Sweet-Parker layer which is often observed between plasmoids in 2D.

the upper or a lower part of the layer dominates.

The classic X-point inflow/outflow picture is usually preserved in 2D in each X-point between plasmoids. In my simulations such a simple picture was not observed, see Fig. 9.

The physical reason for resistivity-independent rate also appears to be different: in the 2D case it relies on the hierarchical formation and ejection of plasmoids (Uzdensky et al. 2010), while in 3D I hypothesize this to be a consequence of turbulence locality, similar to models of reconnection due to ambient turbulence (Lazarian & Vishniac 1999). The difference between 3D reconnection with ambient turbulence and spontaneous reconnection is that in the spontaneous case there is no external agent that drives reconnection and there is no parameter of the amplitude of ambient turbulence as in, e.g., Kowal et al. (2009).

The resistively-independent turbulent reconnection has been already argued for reconnection due to ambient turbulence (Lazarian & Vishniac 1999; Eyink et al. 2011). In this paper I extend this result to the case where reconnection develops spontaneously without an external agent. I demonstrate this by showing that turbulence in the current layer resemble ordinary turbulence and likely to be local in scale. At the sufficiently large Lundquist numbers, the dynamics of large scales, which determines such properties as the bulk reconnection and dissipation rates, will be disconnected from the dynamics on plasma scales and dissipation parameters. It is, therefore, natural to expect reconnection and dissipation rates to go to asymptotic universal values. Whether the locality argument can be applied in 2D is unclear because large plasmoids may couple large and small scales directly.

The reconnection speed in ambient turbulence was argued to be proportional to the kinetic energy density (Lazarian & Vishniac 1999). Our  $v_r = 0.015v_{Ay}$  measurement obtained in absence of ambient turbulence could be seen as a lower limit on fluid reconnection speed in 3D.

## 8. A MODEL FOR THE RECONNECTION RATE

2D theory explaining observed reconnection rate is based on a hierarchical plasmoid model (Uzdensky et al. 2010). This model predicts that the number of plasmoids scales linearly with  $S$  and this hierarchy truncates on the scale of the critical layer. Thus the reconnection rate is just equal to the SP rate at the critical value of  $S$ :  $v_r = v_A S_{crit}^{-1/2}$ . In my picture reconnection is not due to large-scale tearing, but due to turbulence on the edge of the layer. This turbulence, as I showed above is strong and can not be considered a linear stage of any instability.

One of the interesting empirical facts about spontaneous reconnection that I observed in simulations is that the reconnection rate is constant in time and the level of velocity and magnetic perturbations keeps approximately on the same level as well. Can this be reconciled with the turbulent picture, despite the volumetric dissipation rate inside the layer depends on time? The basic scaling for turbulent velocity as a function of turbulent cascade rate is

$$\delta v_l^2 = C_{K,v} \epsilon^{2/3} l^{2/3}, \quad (6)$$

where  $l$  is a scale of interest and I introduced Kolmogorov constant  $C_{K,v}$  that refers to the velocity perturbation, not the total energy spectrum. If we argue that turbulence is driven on the scale of the current layer thickness, i.e.,  $l = \Delta$ , and use Eq. 3 for the dissipation rate, we calculate that  $\delta v_l^2$  indeed does not depend on  $\Delta$  and, therefore, on time:

$$\delta v_l^2 = C_{K,v} w_d^{2/3} v_r^{2/3} v_{Ay}^{4/3}. \quad (7)$$

The fact that  $\delta v_l$  is constant in time is consistent with my numerical measurement. How reconnection rate depends on  $\delta v_l$  is not immediately obvious. One possibility is to use expression for turbulent reconnection rate from Lazarian & Vishniac (1999), but it is not clear how the layer width relates to the time-dependent injection scale  $l$ . Assuming that  $v_r$  depends only on the RMS velocity  $\delta v_l$  at in the current layer, however, in the manner  $v_r = v_{Ay} f(\delta v/v_{Ay})$  I can obtain time-independent rate by substituting Eq. 7 and solving the nonlinear equation

$$v_r = v_{Ay} f(C_{K,v}^{1/2} w_d^{1/3} v_r^{1/3} v_{Ay}^{-1/3}). \quad (8)$$

In particular, using  $v_r \sim M_A^2$  dependence from Lazarian & Vishniac (1999), e.g., choosing  $v_r = C_{LV} \delta v_l^2 / v_{Ay}$  I obtain

$$v_r = C_{LV}^3 C_{K,v}^3 w_d^2 v_{Ay}. \quad (9)$$

The constant  $C_{LV}$  has not been yet precisely measured (c.f. Kowal et al. 2009). The constant  $C_{K,v}$  can be obtained in my simulations and refer to the ordinary Kolmogorov constant, as well as the fraction of the total cascade energy that resides in its kinetic part. Introducing the ratio of kinetic to magnetic energy as  $r_A$ , which is around 0.13 in my simulations, I can estimate  $C_{K,v} = C_K r_A / (1 + r_A) \approx 0.48$  using  $C_K = 4.2$  from Beresnyak (2011). This gives the reconnection rate of  $0.018 C_{LV}^3 v_{Ay}$ , which corresponds to the measured value if  $C_{LV} = 0.94$ .

Interestingly, this expression depends only on the basic properties of well-developed turbulence, dimension-

less numbers  $C_K$  and  $r_A$  and not on the properties of the instability.

## 9. ELECTRON ACCELERATION

The actual dissipation mechanisms of reconnection which will result in observable phenomena are still debated. It is plausible that dissipation in plasmas sometimes results in heating, and sometimes in the acceleration of fast particles. For example, the acceleration on shock fronts starts with particles being pulled out of the thermal pool due to extremely high velocity gradient at the shock front itself. Similarly, solar X-ray flares, which produce accelerated electrons has been brought up as a proof that current layers must have microscopic widths to allow for plasma effects, including parallel electric field, and electron acceleration. The logic is the following: suppose that turbulent reconnection picture is true and current layers are wide compared with plasma scales and electrons only “feel” local turbulent perturbations, in which case electron acceleration will be, basically, stochastic turbulent acceleration. Turbulent acceleration, specifically from the quasilinear theory (Schlickeiser 2002), was calculated to be second order in  $v/c$ , too slow in many practical cases, while acceleration by electric field  $E \sim \mathbf{v}_r \times \mathbf{B}/c$  is first order in  $v/c$  and should dominate.

We recently found that the very basis of the above argument, the claim that turbulent acceleration must be second order is, in fact, not true. In particular, we found analytically that if turbulence is fueled by magnetic energy, like in the case of spontaneous turbulent reconnection, the structure of magnetic and electric fields in this turbulence is such that the average acceleration by curvature drift is positive. This is due to a mathematical relation between the MHD term which is responsible for energy transfer between kinetic and magnetic energy and the term responsible for the curvature drift acceleration (Beresnyak & Li 2016). This does not require extra assumptions such as that particles have to be trapped for considerable time in magnetic islands, in fact the whole volume of turbulence will be the first order accelerator. So, as long as the particle gyro-radius is smaller than the current layer width, the acceleration of these particles will be efficient. The expression for the acceleration rate we derived in Beresnyak & Li (2016),

$$\frac{d\mathcal{E}}{dt} = \mathcal{E}_{\parallel} \frac{8\pi}{B^2} \mathcal{D}, \quad (10)$$

relates it to the energy transfer from magnetic to kinetic energy  $\mathcal{D}$  and the acceleration rate. In ordinary driven turbulence this term is zero, while in spontaneous reconnection it is equal to the half of the total dissipation rate  $\epsilon$ . Since this mechanism results in average acceleration for all particles, all electrons are predicted to be accelerated to approximately the same energy,  $0.35T(L/d_i)^{1/4}$  (Beresnyak & Li 2016), where  $T$  is the thermal energy. The subsequent transition to the regime IV will result in an outflow, particle escape, and additional acceleration due to converging magnetic field lines, which will result in a formation of a power-law tail. It is interesting that X-ray emission during the solar flare indeed feature a thermal component and a power-law tail.

## 10. UNIVERSAL FLUID RESISTANCE TO THIN CURRENT IN THE LIMIT OF ZERO RESISTIVITY

Our result suggests that in the high- $S$  limit all macroscopic properties of reconnection are expressed in terms of macroscopic plasma properties  $\rho$ ,  $v_A$  and  $L$  and independent of microscopic dissipation. This result is quite spectacular considering that individual field lines reconnection does depend on microphysics.

Let us think of the turbulent current layer as a conductor. The electromotive force (EMF) between two points separated by a large distance in  $z$  direction will be expressed as

$$\mathcal{E} = \int \frac{\mathbf{v} \times \mathbf{B}}{c} dz \approx \frac{v_r}{c} B_{y0} L_z, \quad (11)$$

and should be independent of whether we took point inside the current sheet or outside of it. At the same time, the total current flowing through the width  $L_y$  of the current layer will be  $I = (c/4\pi)2B_{y0}L_y$ . Taking the ratio of the two, we obtain the effective resistance of the current layer

$$R = \frac{1}{2} \frac{v_r}{c} \frac{L_z}{L_y} \left( \frac{4\pi}{c} \right) \approx 0.0075 \frac{v_A}{c} \frac{L_z}{L_y} \left( \frac{4\pi}{c} \right) \quad (12)$$

Note that  $R_0 = 4\pi/c$  ( $\sim 376.73\Omega$  in SI units) is known as the impedance of free space, and our final result is independent of microscopic resistivity. Such a resistance will dissipate energy in conductive fluids in spite of the fact that microscopic resistivity of plasma in most astrophysical objects can be considered negligible. In the limit of infinitely heavy plasma,  $v_A/c \rightarrow 0$ , this will result in zero resistance, consistent with ordinary resistance expression proportional to resistivity. For the very light plasma, i.e. the relativistic force-free magnetically dominated limit  $v_A/c = 1$  and the resistance is a sizable fraction of the impedance of free space.

For example, jets in active galactic nuclei are self-contained electromagnetic structures carrying large-scale poloidal current, with at least part of the return poloidal current flowing in a layer separating magnetic pressure-dominated jet and the outside medium (Begelman et al. 1984). Poynting-dominated jet has an impedance of  $\sim 90\Omega$  (Lovelace & Kronberg 2013), and since  $v_A/c \sim 1$  for rarefied electron-positron plasma, we can estimate that jets with aspect ratios of  $L_z/L_y > 650$  will dissipate a sizable fraction of their energy in a outer current layer, due to this layer's fundamental fluid resistance. Whether this will result in an outer layer's visibility is an open question, but considering the result of the previous section, the first order acceleration of particles and non-thermal emission from this layer is highly likely.

Another example is dissipation in pulsar magnetospheres, which feature the return current layer in the equatorial plane beyond the light cylinder Uzdensky & Spitkovsky (2012). The current layer separating open and closed field lines within light cylinder (see, e.g., Arons 2011) can also result in acceleration.

## 11. DISCUSSION

Our simulations clearly demonstrate that turbulence must be a part of high-Lundquist reconnection, e.g., as-

trophysical reconnection. Quite importantly, this turbulence is not random, but contains non-trivial correlations that comes from the fact that energy is transferred from magnetic to kinetic, these correlations likely to result the efficient particle acceleration (Beresnyak & Li 2016), which can help explaining why reconnection on the Sun results in powerful X-ray flares. Observational evidence favoring spontaneous turbulent reconnection include magnetospheric observations that showed an enhanced level of turbulence inside current sheets (Matsumoto et al. 2003; Cattell et al. 2005).

Many astrophysical objects, such as the interstellar medium in our Galaxy, feature relatively high level of ambient turbulence and the reconnection is argued to be fast (Lazarian & Vishniac 1999) due to the existing magnetic field stochasticity. In highly magnetized environments, such the solar surface or the pulsar wind nebulae, the velocity of ambient turbulence may be tiny compared to the local Alfvén speed and the turbulence, spontaneously generated by the current sheet, and fueled by the reconnecting field itself is more important. More qualitatively, if  $M_A = \delta v/v_A < \sqrt{0.015} \approx 0.12$ , spontaneous reconnection will dominate. Future parameter study in simulations with Lundquist number above critical and varying level of ambient turbulence should clarify the transition between turbulent reconnection due to ambient turbulence and spontaneous reconnection. So far, simulations with driven turbulence had  $S < 10^4$ , so the non-driven case was still consistent with Sweet-Parker picture (Kowal et al. 2009), with resistive rate higher than 0.015 that I measured in this paper.

Currently, two completely opposite ways to explain fast spontaneous reconnection exist. First is the model that relates reconnection rate to the critical Lundquist number, i.e. the claim that reconnection rate depends on the stability to linear resistive tearing. This gives dimensionless rate of  $S_{crit}^{-1/2}$  (Uzdensky et al. 2010). The second relates reconnection to the inherent properties of strong turbulence and gives the reconnection rate of  $C_K^3 r_A^3 / (1 + r_A)^3$  (this paper). Both pictures reasonably agree with the measurement, but hard to reconcile with each other. One way to connect these pictures is to imagine that turbulence produces constant anomalous resistivity which brings effective Lundquist number to or below critical value, just to barely suppress tearing. The counter-argument to this is that the linear stability studies have only been performed in the laminar SP regime and the large value of  $S_{crit}$  is the result of a rather non-trivial interplay between resistive tearing rate  $\sim \eta^{1/2}$ , and thinning of the current layer. In a non-laminar case it is easy to argue for  $S_{crit} \sim 1$ , but hard to argue for  $S_{crit} \sim 10^4$ .

In stationary reconnection with speed  $v_r$  that developed outflow with speed  $v_{out}$  and reach quasi-stationary state as in Fig. 1 panel (IV) the inflow speed is balanced by the outflow  $v_{in} = v_r$ . In this case the current layer width also reach stationary value of  $\Delta = Lv_r/v_{out}$ , neglecting compressibility. Similar to the cascade locality argument, e.g., the argument why  $v_r$  should be independent on  $S$ , the outflow speed also must be a fraction of  $v_A$ . It is not necessarily equals to  $v_A$  as it is often assumed. The outflow develops under the force of magnetic tension from  $B_y$  component but we showed that a



sizable fraction of this energy is dissipated and not converted into kinetic motion. We expect the outflow speed to be a sizable fraction of the  $v_{Ay}$ , this fraction being lower by a factor of  $\sim \sqrt{1-0.4} \approx 0.77$ , where  $w_d \approx 0.4$  is a dissipation factor that we found in this paper.

The reconnection rate could be affected by the presence of an outflow in regime IV. Increasing the box size will allow larger-scale fluid motions which could emulate the outflow effect locally, this also correspond to higher  $S$ . We showed that with increasing  $S$  the reconnection rate goes to a constant. This is probably associated with the fact that most of the activity which results in a growth of the current layer happens on the boundary. Likewise, the simulation naturally included the effects of the local outflows that develop on larger and larger scales as reconnection progresses, while the reconnection rate stay

relatively stable (Fig. 3).

It is also worth mentioning that the fraction of the dissipated energy that we measured,  $w_d \approx 0.4$ , will limit the compression ratio of the current layer. Previously it was thought that most of the magnetic energy during reconnection could be spent to accelerate the outflow jet, which is why the outflow speed was always estimated being equal to Alfvén speed (see above). In this case the compression ratio may be arbitrarily high for low beta plasmas, going as  $1/\beta$ . In our case the compression ratio will be limited to  $1/w_t(\gamma - 1) \approx 3.8$  for monoatomic gas.

**Acknowledgements** I am grateful to Alex Schekochihin, Nuno Loureiro, Fan Guo, Alex Lazarian, Ethan Vishniac, Homa Karimabadi, Bill Daughton and Hui Li for fruitful discussions. Computations were performed on NICS Kraken with XSEDE allocation TG-AST110057 and on LANL institutional computing resources.

#### REFERENCES

- Arons, J. 2011, in *High-Energy Emission from Pulsars and their Systems*, ed. D. F. Torres & N. Rea, 165
- Begelman, M. C., Blandford, R. D., & Rees, M. J. 1984, *Reviews of Modern Physics*, 56, 255
- Beresnyak, A. 2011, *Phys. Rev. Lett.*, 106, 075001
- 2012, *MNRAS*, 422, 3495
- 2014, *ApJ*, 784, L20
- Beresnyak, A., & Lazarian, A. 2009, *ApJ*, 702, 460
- Beresnyak, A., & Lazarian, A. 2015, in *Astrophysics and Space Science Library*, Vol. 407, *Magnetic Fields in Diffuse Media*, ed. A. Lazarian, E. M. de Gouveia Dal Pino, & C. Melioli, 163
- Biskamp, D. 1986, *Physics of Fluids*, 29, 1520
- 2000, *Magnetic Reconnection in Plasmas* (UK: Cambridge)
- 2003, *Magnetohydrodynamic Turbulence* (Cambridge: Cambridge University Press)
- Brandenburg, A., Kahniashvili, T., & Tevzadze, A. G. 2015, *Physical Review Letters*, 114, 075001
- Cattell, C., Dombek, J., Wygant, J., Drake, J. F., Swisdak, M., et al. 2005, *Journal of Geophysical Research (Space Physics)*, 110, 1211
- Che, H., Drake, J. F., & Swisdak, M. 2011, *Nature*, 474, 184
- Cho, J., & Vishniac, E. T. 2000, *ApJ*, 538, 217
- Daughton, W., Roytershteyn, V., Albright, B., Karimabadi, H., Yin, L., & Bowers, K. 2009, *Physical review letters*, 103, 65004
- Daughton, W., Roytershteyn, V., Karimabadi, H., Yin, L., Albright, B. J., Bergen, B., & Bowers, K. J. 2011, *Nature Physics*, 7, 539
- Dere, K. P. 1996, *The Astrophysical Journal*, 472, 864
- Drake, J. F., Swisdak, M., Che, H., & Shay, M. A. 2006, *Nature*, 443, 553
- Dungey, J. W. 1961, *Physical Review Letters*, 6, 47
- Eyink, G., Vishniac, E., Lalescu, C., Aluie, H., Kanov, K., et al. 2013, *Nature*, 497, 466
- Eyink, G. L., Lazarian, A., & Vishniac, E. T. 2011, *ApJ*, 743, 51
- Goldreich, P., & Sridhar, S. 1995, *ApJ*, 438, 763
- Huang, Y.-M., & Bhattacharjee, A. 2010, *Physics of Plasmas*, 17, 062104
- 2016, *ApJ*, 818, 20
- Kowal, G., Lazarian, A., Vishniac, E. T., & Otmianowska-Mazur, K. 2009, *ApJ*, 700, 63
- Lazarian, A., Beresnyak, A., Yan, H., Opher, M., & Liu, Y. 2008, in *From the Outer Heliosphere to the Local Bubble* (Springer New York), 387–413
- Lazarian, A., & Vishniac, E. T. 1999, *ApJ*, 517, 700
- Loureiro, N. F., Samtaney, R., Schekochihin, A. A., & Uzdensky, D. A. 2012, *Physics of Plasmas*, 19, 042303
- Loureiro, N. F., Schekochihin, A. A., & Cowley, S. C. 2007, *Physics of Plasmas*, 14, 100703
- Lovelace, R. V. E., & Kronberg, P. P. 2013, *MNRAS*
- Matsumoto, H., Deng, X. H., Kojima, H., & Anderson, R. R. 2003, *GRL*, 30, 060000
- Oishi, J. S., Mac Low, M.-M., Collins, D. C., & Tamura, M. 2015, *ApJ*, 806, L12
- Parker, E. 1994, *Spontaneous current sheets in magnetic fields: with applications to stellar x-rays* (USA: Oxford University Press)
- Parker, E. N. 1957, *JGR*, 62, 509
- Priest, E., & Forbes, T. 2000, UK: Cambridge
- Schekochihin, A. A., Cowley, S. C., Dorland, W., Hammett, G. W., Howes, G. G., Quataert, E., & Tatsuno, T. 2009, *ApJ*, 182, 310
- Schlickeiser, R. 2002, *Cosmic Ray Astrophysics* (Berlin: Springer)
- Sweet, P. A. 1969, *Ann. Rep. A&A*, 7, 149
- Syrovatskii, S. 1971, *Sov. phys. JETP*, 33, 933
- Uzdensky, D., Loureiro, N., & Schekochihin, A. 2010, *Physical review letters*, 105, 235002
- Uzdensky, D. A., & Spitkovsky, A. 2012, *ArXiv e-prints*